J. Fluid Mech. (1975), *vol.* 72, *part* 3, *pp.* 529–540
Printed in Great Britain

On the movement of slender bodies near plane boundaries at low Reynolds number

By D. F. KATZ†, J. R. BLAKE‡
Department of Applied Mathematics and Theoretical Physics, University of Cambridge
AND S. L. PAVERI-FONTANA
Istituto di Meccanica Razionale, Universitá di Bari, Italy

(Received 21 February 1975)

Normal and tangential resistance coefficients are calculated for a rigid slender body close to a planar no-slip boundary or midway between and close to two such boundaries. The important length scale is found to be the separation distance from the boundaries, and the forces per unit length acting on the slender body are approximately constant along most of its length. Owing to the presence of the walls, the ratio of the normal and tangential resistance coefficients can be greater than 2, its maximum limiting value in the infinite-fluid case. Applications to the movements of flagellated micro-organisms are discussed.

1. Introduction

This paper studies low Reynolds number translational movements of a rigid straight slender body in close proximity to a single plane wall or two such walls. The object of this study is the development of analytical relationships between velocities of translation along principal body axes and average resistive forces per unit body length acting in response to those motions. Such information is of particular interest in describing the hydrodynamics of movement of flexible active slender bodies, such as the flagella and cilia of aquatic micro-organisms. There a useful hydrodynamical approach is to introduce the 'resistive force' approximation

$$\langle F_i \rangle = -C_i v_i \quad \text{(no summation convention)}; \tag{1.1}$$

cf. Gray & Hancock (1955), Lighthill (1975, chap. 3) and Pironneau & Katz (1974). In (1.1), $\langle \mathbf{F} \rangle$ is the net force per unit length acting at a particular point along the axis of a slender body, $\mathbf{v}$ is the velocity of that point relative to the fluid at infinity and the C_i are coefficients of proportionality, conveniently termed 'resistance coefficients'; the i direction is along one of the three principal body axes at that point. Starting with (1.1) and a knowledge of the C_i, and invoking momentum conservation principles for the entire slender body as

† Present address: Department of Mechanical Engineering, University of California, Berkeley.

‡ Present address: CSIRO Division of Mathematics and Statistics, Canberra, Australia.

FIGURE 1. Simulation of a curved slender body by a contiguous succession of shorter straight slender bodies.

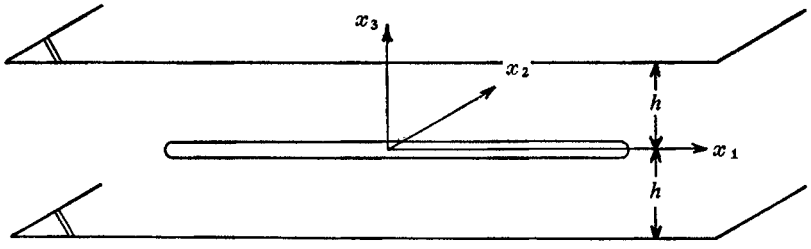

FIGURE 2. Slender body near infinite plane wall(s).

necessary, information regarding propulsive and fluid field velocities, rates of working and viscous bending moments can be obtained.

The details of the shape of the slender body and its undulations are contained in the resistance coefficients C_i. Strictly speaking, these depend upon the position along the flagellum and time. Development of expressions for the C_i appropriate to undulations of finite amplitude is a difficult task indeed. The principal difficulty is the fact that the forces acting at any point along the body axis depend not just upon the movements of that point, but simultaneously upon the movements of all other points along the axis, a phenomenon commonly termed the 'neighbouring effect'. This difficulty is alleviated if only undulations of small amplitude are considered, so that the neighbouring effect is negligible. In such a case it is instructive to view the slender body as a segmented contiguous assemblage of short, rigid, straight slender bodies; see figure 1. If end effects on the overall body are neglected, then a single value of C_i can be used for all sub-bodies. It is this situation, then, which motivates our study.

We consider a cylindrical body of radius r_0 and length $2l$ such that $r_0 \ll l$. The body axis translates while remaining in a plane situated at a distance h from either a single infinite plane wall, or two such walls; see figure 2. In all cases $r_0 \ll h \ll l$. For a single wall, we represent the flow field by a distribution of appropriate singularities located along the body axis and its image line. Aspects of this problem have been studied numerically by Blake (1974), and his results will be of comparative interest here. In the case of two walls, we represent the flow field using an application of the Faxén (1923) technique introduced by de Mestre (1973).

2. Slender-body movements near a single plane wall

In this section we consider a slender body situated a distance h from a single stationary plane wall; cf. figure 2. The slender body may translate in the x_1, x_2 or x_3 direction, i.e. longitudinally, transversely in a plane parallel to the wall or

transversely in a plane normal to the wall, respectively. For such motions, it is convenient to represent the velocity field in the fluid using a distribution of appropriate singularities along the centre-line of the body. Thus we can pose the following integral equation for the velocity $\mathbf{u}(\mathbf{x})$:

$$u_i(\mathbf{x}) = \int_{-l}^{l} G_{ij}(\mathbf{x}, s)\, F_j(s)\, ds, \tag{2.1}$$

where $\mathbf{F}(s)$ is the force per unit length acting on the body and $G_{ij}(\mathbf{x}, s)$ is the Green's function appropriate to the geometry of the problem (and the no-slip boundary condition). Here

$$G_{ij}(\mathbf{x}, s) = \frac{1}{8\pi\mu}\left\{\left[\frac{\delta_{ij}}{r} + \frac{r_i r_j}{r^3}\right] + \left[-\left(\frac{\delta_{ij}}{R} + \frac{R_i R_j}{R^3}\right)\right.\right.$$
$$\left.\left. + 2h(\delta_{j\alpha}\delta_{\alpha k} - \delta_{j3}\delta_{3k})\frac{\partial}{\partial R_k}\left(\frac{hR_i}{R^3} - \frac{\delta_{i3}}{R} - \frac{R_i R_3}{R^3}\right)\right]\right\}, \quad \alpha = 1, 2, \tag{2.2}$$

where $r = [(x_1 - s)^2 + x_2^2 + x_3^2]^{\frac{1}{2}}$, $R = [(x_1 - s)^2 + x_2^2 + (x_3 + 2h)^2]^{\frac{1}{2}}$ and μ is the viscosity. The first term in square brackets in (2.2) represents a distribution of Stokeslets along the centre-line of the body, while the second square-bracketed term is the image system needed to satisfy the no-slip condition on the plane boundary; cf. Blake (1971) and Blake & Chwang (1974). This system consists of Stokeslets of equal magnitude but opposite sign to those on the body axis, Stokes doublets of strength $2h$ times that of the Stokeslets, and source doublets of strength $2h^2$ times the Stokeslet strength. In (2.2) we have omitted additional singularities as they are of higher order.

We seek an approximate analytic solution to (2.1) appropriate to the restrictions $r_0 \ll h \ll l$ and the boundary condition $\mathbf{u} = \mathbf{U}$ on $r = r_0$. Asymptotic approaches to the solution of this equation, primarily for an isolated slender body, have received considerable attention in recent years; cf. Tillet (1970), Batchelor (1970) and Cox (1970). We shall briefly outline our approach; for more details of the general problem the reader is referred to the above references. We wish to evaluate (2.1) on the surface of the slender body, which in cylindrical co-ordinates is (x_1, r_0, θ). Noting that (2.1) is singular in the limit $r_0 \to 0$, we conclude that the major contribution to the integral occurs in the vicinity of the point $s = x_1$. Thence we rewrite (2.1) as

$$u_i(x_i, \theta) = F_j(x_1)\int_{-l}^{l} G_{ij}(\mathbf{x}, s)\, ds + \int_{-l}^{l} G_{ij}(\mathbf{x}, s)\,[F_j(s) - [F_j(x_1)]\, ds, \tag{2.3}$$

where now $r = [(x_1 - s)^2 + r_0^2]^{\frac{1}{2}}$ and $R = [(x_1 - s)^2 + r_0^2 + 4r_0 h \sin\theta + 4h^2]^{\frac{1}{2}}$. Since we are interested here in quantifying the wall effect, we shall obtain an approximate solution to (2.3) by considering only the first term on the right-hand side. Once the magnitude and general analytic nature of the effect are known, a more sophisticated asymptotic expansion of the entire problem can follow. We note that, if $F_i(x_1)$ is approximately constant along most of the length of the slender body, then our expressions for the resistance coefficients will be reasonably accurate. This is not, in fact, the case for a slender body translating in an

infinite fluid. Thus it remains for us to evaluate the integral of the Green's function along the body. For convenience, we shall write this integral as the sum $I_{ij}+J_{ij}$, where I_{ij} is the contribution from the singularities on the body axis and J_{ij} is due to the images. Thence

$$u_i(x_1,\theta) \simeq (F_j(x_1)/8\pi\mu)\,(I_{ij}+J_{ij}). \tag{2.4}$$

The integrals I_{ij} are familiar from the theory of isolated slender bodies, and are simplified by applying the slenderness limit $r_0/l \ll 1$. For example,

$$\begin{aligned}\int_{-l}^{l} \frac{ds}{[(x_1-s)^2+r_0^2]^{\frac{1}{2}}} &= \sinh^{-1}\left(\frac{l-x_1}{r_0}\right)+\sinh^{-1}\left(\frac{l+x_1}{r_0}\right)\\ &= \ln\left[4\left(\frac{l^2-x_1^2}{r_0^2}\right)\right]+O\left(\frac{r_0}{l\pm x_1}\right)^2,\end{aligned} \tag{2.5}$$

the notion being that contributions from points near the end points $x_1 = \pm l$ are less significant, and can be neglected at this level of approximation. In previous asymptotic expansions for the infinite-fluid case, it has been common to expand the logarithm in (2.5) into $2\ln(2l/r_0)+\ln[1-(x_1/l)^2]$, and to take as a first approximation the first of these terms. It is not necessary, however, for us to do this here, as the images in the wall will provide a convenient cancellation. The following approximate values are thus obtained:

$$\left.\begin{aligned} &I_{11} = 2\ln\frac{4(l^2-x_1^2)}{r_0^2}-2, \quad I_{22} = \ln\frac{4(l^2-x_1^2)}{r_0^2}+1+\cos 2\theta,\\ &I_{33} = \ln\frac{4(l^2-x_1^2)}{r_0^2}+1-\cos 2\theta,\\ &I_{12} = I_{21} = 0, \quad I_{23} = I_{32} = \sin 2\theta, \quad I_{13} = I_{31} = 0.\end{aligned}\right\} \tag{2.6}$$

The terms in $\cos 2\theta$ and $\sin 2\theta$ represent variations around the cross-section of the body and can be removed either by averaging around that cross-section, or by introducing source doublets of appropriate strengths along the centre-line of the body. Note that such doublets do not significantly influence the flow field (and therefore the boundary conditions) at the wall, provided that $r_0/h \ll 1$. Consequently their presence does not necessitate inclusion of any additional image singularities.

The mathematical procedure for obtaining the J_{ij} is very similar to that for the I_{ij}, i.e. the limits $r_0 \ll h \ll l$ are applied to the integrals. It is instructive to decompose the results into the separate contributions of the image Stokeslets, Stokes doublets and source doublets; see table 1. For $i \neq j$, $J_{ij} = 0$ to this order of approximation. The flow field due to the image system does not vary around the cross-section of the body. A physical discussion of the separate effects of the image singularities is contained in Lighthill (1975, chap. 7).

We can now evaluate the net forces per unit length acting on the body owing to separate translations in the x_1, x_2, and x_3 directions. In particular, addition of the results in (2.6) and table 1 indicates that to this order of approximation the *local* force per unit length is constant along the body, and is therefore equal

	Stokeslets	Stokes doublets	Source doublets
J_{11}	$-2\ln[(l^2-x_1^2)/h^2]+2$	0	0
J_{22}	$-\ln[(l^2-x_1^2)/h^2]$	-2	1
J_{33}	$-\ln[(l^2-x_1^2)/h^2]-2$	-2	1

TABLE 1

to the *average* force. The results here are then conveniently expressed in terms of resistance coefficients $C_i = 8\pi\mu/(I_{ij}+J_{ij})$ [cf. (1.1)] as

$$C_1 = \frac{2\pi\mu}{\ln(2h/r_0)}, \quad C_2 = \frac{4\pi\mu}{\ln(2h/r_0)}, \quad C_3 = \frac{4\pi\mu}{\ln(2h/r_0)-1}. \tag{2.7}$$

3. Slender-body movements midway between two plane walls

In this section we consider a slender body whose centre-line remains in a plane a distance h from stationary plane walls above and below it; cf. figure 2. The body may translate in the x_1 or x_2 direction, i.e. either longitudinally or transversely parallel to the walls. Here it is convenient to study the flow field by employing the technique introduced by Faxén (1923; see also Happel & Brenner 1965, pp. 323–324) in connexion with a sphere falling between two parallel walls. The technique develops a sum of integral expressions for the velocity field which are appropriate to the solid boundaries present. However a straightforward physical interpretation, such as that in §2, is not possible. The Faxén method has been employed by de Mestre (1973) to study the slender-body movements mentioned above in the case where $h \gg l$. Our analysis proceeds from the stage in de Mestre's analysis where an assumption regarding the magnitude of h becomes necessary. In that analysis a relation is developed between the velocity U_2 of transverse translation by the body and the transverse force $F_2(s)$ per unit length, i.e. the Stokeslet strength, acting on the body. This relation can be written as

$$U_2 = \frac{1}{8\pi\mu}\left\{\int_{-l}^{l}\frac{1+\cos^2\theta}{r_0}F_2(s)\,ds + \frac{1}{2\pi}\int_{-\infty}^{\infty}d\alpha\int_{-\infty}^{\infty}d\beta\int_{-l}^{l}ds \right.$$
$$\left. \times \exp[i(\alpha x_1 - \alpha s + \beta r_0\sin\theta)]\,G(\alpha,\beta,x_3)\,F_2(s)\right\}. \tag{3.1}$$

It proves necessary to use the complete expression for $G(\alpha,\beta,x_3)$, which can be derived from de Mestre's analysis as

$$G(\alpha,\beta,x_3) = e^{-kx_3}\left\{\frac{-2\beta^2h(e^{2kh}-khe^{2kh}-1-kh)}{k^2(e^{2kh}+1)(e^{-2kh}+4kh-e^{2kh})} - \frac{2}{k(e^{2kh}+1)}\right.$$
$$\left. + \frac{\beta^2(1+kx_3)}{k^3(e^{2kh}+1)} + \frac{2x_3\beta^2h(e^{2kh}-1)}{k(e^{2kh}+1)(e^{-2kh}+4kh-e^{2kh})}\right\}$$
$$+ e^{kx_3}\left\{\frac{-2\beta^2h(e^{2kh}-khe^{2kh}-1-kh)}{k^2(e^{2kh}+1)(e^{-2kh}+4kh-e^{2kh})} - \frac{2}{k(e^{2kh}+1)}\right.$$
$$\left. + \frac{\beta^2(1-kx_3)}{k^3(e^{2kh}+1)} + \frac{2x_3\beta^2h(e^{2kh}-1)}{k(e^{2kh}-1)(e^{-2kh}+4kh-e^{2kh})}\right\}, \tag{3.2}$$

with $k = (\alpha^2+\beta^2)^{\frac{1}{2}}$. Now (3.1) may be regarded as the counterpart here of the transverse component of (2.1). Accordingly, we can consider a lowest-order approximate simplification of (3.1) by effectively taking $F_2(s) \simeq F_2(x_1)$ and writing it as a factor outside the integrands. The θ dependence inherent in the presence of $G(\alpha, \beta, x_3)$ in the second integrand of (3.1) is analogously a higher-order effect. It can be removed by expanding $G(\alpha, \beta, x_3)$ in a Taylor series about $x_3 = 0$ and observing that

$$G(\alpha, \beta, x_3) = G(\alpha, \beta, 0) + O(r_0/h)$$

is a sufficient approximation here. The θ dependence in the first integral is removed as in § 2. Invoking slenderness considerations as before, it follows that

$$U_2 \simeq \frac{F_2(x_1)}{8\pi\mu}\left\{\ln\left[\frac{4(l^2-x_1^2)}{r_0^2}\right] + 1 - \frac{1}{\pi}\int_{-\infty}^{\infty}\int_{-\infty}^{\infty} e^{i\alpha x_1} G(\alpha, \beta, 0)\frac{\sin \alpha l}{\alpha} d\alpha d\beta\right\}. \quad (3.3)$$

Note that (3.3) was obtained by de Mestre in the limit of large separation $h \gg l$. Now, integrating with respect to x_1 along the body to obtain an average force per unit length, we obtain

$$U_2 \simeq \frac{\langle F_2\rangle}{8\pi\mu}\left\{2\ln\frac{2l}{r_0} + 1 + \int_{-1}^{1} \ln(1-\eta^2)\, d\eta - \frac{h}{\pi l}\int_0^{2\pi}\int_0^{\infty} \frac{\sin^2(Kl\cos\phi/h)}{K^2\cos^2\phi} H(K,\phi)\, d\phi\, dK\right\}, \quad (3.4)$$

with $\alpha = k\cos\phi$, $\beta = k\sin\phi$, $K = kh$ and

$$H(K,\phi) = \frac{1}{(e^{2k}+1)}\left\{4 - \sin^2\phi\left[2 - \frac{4K(e^{2K} - Ke^{2K} - 1 - K)}{e^{-2K} + 4K - e^{2K}}\right]\right\}. \quad (3.5)$$

The procedure for the case of longitudinal translation in the x_1 direction is analogous. There we obtain

$$U_1 \simeq \frac{\langle F_1\rangle}{8\pi\mu}\left\{4\ln\frac{2l}{r_0} - 2 + 2\int_{-1}^{1} \ln(1-\eta^2)\, d\eta - \frac{h}{\pi l}\int_0^{2\pi}\int_0^{\infty} \frac{\sin^2[(Kl/h)\sin\phi]}{K^2\sin^2\phi} H(K,\phi)\, d\phi\, dK\right\}. \quad (3.6)$$

It remains for us to obtain analytical approximations for the final integrals in (3.4) and (3.6), which we term respectively $W_2(\lambda)$ and $W_1(\lambda)$, with $\lambda = l/h$.

In (3.4) let $\xi = \cos\phi$ and in (3.6) let $\xi = \sin\phi$. Then

$$W_i(\lambda) = \frac{4}{\pi\lambda}\int_0^1 \frac{d_\xi}{(1-\xi^2)^{\frac{1}{2}}}\int_0^{\infty} \frac{\sin^2 K\lambda\xi}{K^2\xi^2}[f_{1,i}(K) + \xi^2 f_{2,i}(K)]\, dK, \quad i = 1, 2, \quad (3.7)$$

where

$$f_{1,2}(K) = \frac{1}{1+e^{2K}}\left\{2 + 4K\left[\frac{e^{2K}(K-1)+(K+1)}{e^{2K} - 4K - e^{-2K}}\right]\right\}, \quad (3.8)$$

$$f_{2,2}(K) = \frac{1}{1+e^{2K}}\left\{2 - 4K\left[\frac{e^{2K}(K-1)+(K+1)}{e^{2K} - 4K - e^{2K}}\right]\right\} = -2f_{2,1}(K), \quad (3.9)$$

$$f_{1,1}(K) = 2/(1+e^K). \quad (3.10)$$

Starting from this form, we obtain in the appendix the following approximate expressions for W_1 and W_2:

$$W_1 = 2\ln(l/h) + 2\{\ln(2m) - A - \tfrac{1}{2} + \mathscr{J}_m[f_{1,1}]\} + O(h/l)^{\frac{1}{2}}, \tag{3.11}$$

$$W_2 = 2\ln(l/h) + 2\{\ln(2m) - A + 1 + \mathscr{J}_m[f_{1,2}]\} + O(h/l)^{\frac{1}{2}}, \tag{3.12}$$

where

$$A = \int_0^\infty \frac{\ln\eta}{\eta} J_1(\eta)\,d\eta = -0{\cdot}27036$$

and

$$\mathscr{J}_m[f] = \int_0^m \frac{f(K)-f(0)}{K}dK + \int_m^\infty \frac{f(K)}{K}dK. \tag{3.13}$$

$J_1(\eta)$ is the first-order ordinary Bessel function of the second kind. Here m is any positive number; for the functions $f_{1,j}$ it may readily be shown that $\mathscr{J}_m[f]$ exists and that $\ln m + \mathscr{J}_m[f]$ is independent of m. The latter has been evaluated numerically for the functions of interest here.

Returning to (3.4) and (3.6), the final approximate expressions for the resistance coefficients C_1 and C_2 can be written as

$$C_1 = \frac{2\pi\mu}{\ln(2h/r_0) - 0{\cdot}453}, \quad C_2 = \frac{4\pi\mu}{\ln(2h/r_0) - 1{\cdot}609}. \tag{3.14), (3.15}$$

4. Discussion

Some comments are warranted on the accuracy of our approximate solutions. In the theory of isolated slender bodies, retention of only the first term in (2.3) is tantamount to accepting errors $O(\ln(2l/r_0))^{-2}$. The slenderness approximations used in obtaining I_{ij} are correct to $O(r_0/l)$, and are thus within the above approximation. When a nearby wall is present, however, (2.7) indicate that the resistance coefficients become $O(\ln(2h/r_0))^{-1}$, with errors of higher order in approximating (2.3). Errors incurred in obtaining J_{ij} are no worse than $O(r_0/h)$, and are thus acceptable. Indeed, when $h/l \ll 1$, asymptotic expansions in powers of $\ln(2h/r_0)^{-1}$ are suggested.

Very near a wall, then, the separation distance h, rather than the body length $2l$, becomes the important length scale. We may presume that, in the presence of two walls, errors of comparable magnitude arise in the development of (3.4) and (3.6). As indicated in the appendix, our asymptotic calculation of the integrals W_1 and W_2, which occur in (3.4) and (3.6), is correct to $O(r_0/h)^{\frac{1}{2}}$, and is therefore acceptable.

It is of interest to compare our approximate analytic results (2.7) for C_1, C_2 and C_3 with the numerical computations of Blake (1974). He presented two approaches. The first is similar to that of Batchelor (1970), with the addition of an $O(\ln 2l/r_0)^{-2}$ iterative correction to the contribution of the body Stokeslets (though not the image system). Consequently there is a slight x_1 dependence in the ratios F_i/U_i, apart from the arguably neglectable singularities at the ends of the body $x_1 = \pm l$. As was indicated in Blake (1974), this expansion approach is not suitable when a slender body becomes close to a plane boundary, particularly for motion towards the boundary. For $h/l = 0{\cdot}1$, however, these ratios are

	C_1/μ	C_2/μ	C_3/μ
Blake: partial numerical solution	2·183	4·093	4·366
Blake: complete numerical solution	—	4·912	8·868
Present work	2·729	5·458	9·647

TABLE 2

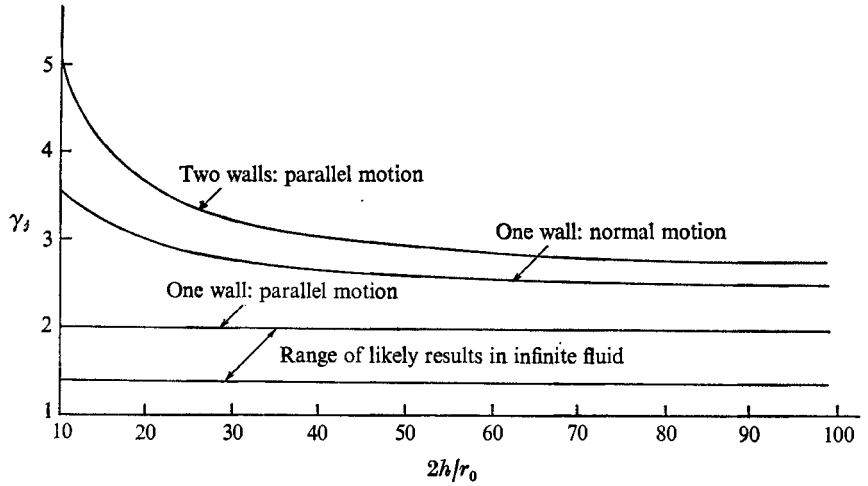

FIGURE 3. Dependence of $\gamma_j = C_j/C_1$ ($j = 2, 3$) upon separation distance h; r_0 is the flagellum radius.

invariant along most of the body, and suitable for use in computing effective resistance coefficients. As a second approach, Blake solved the integral equation (2.1) directly, via a matrix inversion technique. Transverse movements in the x_2 or x_3 direction were considered. In the limit of small clearance, say $h/l = 0{\cdot}1$, these latter results indicated significantly higher resistive forces than did the first approach. Interestingly, comparison of effective resistance coefficients with our analytical results indicates much better agreement with the second approach. For example, letting $r_0/l = 0{\cdot}02$ and $h/l = 0{\cdot}1$, we obtain the results in table 2.

With regard to the self-propulsion of flagellated micro-organisms, the parameters of primary interest are the ratios of transverse and longitudinal resistance coefficients, $\gamma_1 \equiv C_2/C_1$ and $\gamma_2 \equiv C_3/C_1$. Of course, use of γ_2 here to characterize flagellar undulations in a plane normal to a wall is a considerable simplification since it requires that h be effectively the same for all points on the body centre-line. Our inclusion of γ_2 here is nevertheless consistent with the small amplitude restrictions in the entire analysis, and enables us to compare the relative importance of undulations normal and parallel to a wall. In figure 3 we have plotted values of γ_1 and γ_2 for motion near a single wall and values of γ_1 for motion midway between two nearby walls. Note that in the single-wall case γ_1 exactly equals 2 while $\gamma_2 > 2$, but that $\gamma_1 > 2$ in the case of two walls. Our current understanding of the hydrodynamics of the propulsion of isolated flagella suggests a value of γ_1 in the neighbourhood of 1·8. Thus the presence of nearby

walls has a significant influence on propulsive velocity, which, roughly speaking, increases as γ. Since the coefficients themselves increase as h decreases, the rate of working and the distribution of the viscous bending moments also increase in magnitude as a wall is approached. Quantitative details of these responses to a wall are contained in Katz & Blake (1974). When the wall separation diminishes to the order of a body length, the wall effect becomes significant.

It is appropriate to remark again in closing that our results can only be strictly applied to slender-body undulations of small amplitude. In fact *all* derivations of expressions for resistance coefficients to date are based upon this assumption, even though they have often been applied to undulations of finite amplitude. The physiological application of all these small amplitude theories, while valuable, is nonetheless restricted. Indeed, our understanding of flagellar and ciliary movement and function has reached a level where finite amplitude theories are needed. We hope that they will be forthcoming.

DFK acknowledges the support of a Population Council postdoctoral fellowship and an NIH research grant (HD8018). SLP-F participated in this study under the auspices of the CNR, Italy.

Appendix 1. Asymptotic evaluation of $W_1(\lambda)$ and $W_2(\lambda)$ for $\lambda \gg 1$

Preliminary remarks

Let us rewrite (3.7) as

$$W_1(\lambda) = w_{1,1}(\lambda) - \tfrac{1}{2}w^*(\lambda), \quad W_2(\lambda) = w_{1,2}(\lambda) + w^*(\lambda), \tag{A 1}$$

where

$$w_{1,i}(\lambda) = \frac{4}{\pi\lambda}\int_0^\infty \frac{f_{2,i}(K)}{K^2}\,dK \int_0^1 \frac{\sin^2 K\lambda\xi}{\xi^2(1-\xi^2)^{\frac{1}{2}}}\,d\xi, \quad i = 1, 2, \tag{A 2}$$

$$w^*(\lambda) = \frac{4}{\pi\lambda}\int_0^\infty \frac{f_{2,2}(K)}{K^2}\,dK \int_0^1 \frac{\sin^3 K\lambda\xi}{(1-\xi^2)^{\frac{1}{2}}}\,d\xi. \tag{A 3}$$

We note that the functions $f_{1,2}(K)$, $f_{2,2}(K)$ and $f_{1,1}(K)$, given in (3.8)–(3.10), satisfy the conditions

$$f(K) = 1 + O(K) \quad \text{for} \quad K \to 0^+, \tag{A 4}$$

$$\left|\int_0^\infty f(K)\,dK\right| < \infty. \tag{A 5}$$

Letting $f(K) = 1 + K\psi(K)$, for any $m > 0$

$$\left|\int_0^m \psi(K)\,dK\right| < \infty, \quad \left|\int_0^m \frac{\psi(K)}{K^{\frac{1}{2}}}\,dK\right| < \infty, \tag{A 6}$$

$$\int_m^\infty \left|\frac{f(K)}{K}\right| dK = \int_m^\infty \frac{1 + K\psi(K)}{K}\,dK < \infty. \tag{A 7}$$

However, note that the integrals

$$\int_m^\infty \psi(K)\,dK, \quad \int_0^m \frac{\psi(K)}{K}\,dK$$

do not exist. Note also that the functions $f(K)$ and $\psi(K)$ are bounded for

$$0 < K < \infty.$$

In the asymptotic estimates below, we use the following results:

$$\frac{4}{\pi}\int_0^1 \frac{\sin^2\eta\xi}{(1-\xi^2)^{\frac{1}{2}}}d\xi = 1-J_0(2\eta), \tag{A 8}$$

$$\frac{4}{\pi\eta}\int_0^1 \frac{\sin^2\eta\xi}{\xi^2(1-\xi^2)^{\frac{1}{2}}}d\xi = 2\int_0^{2\eta}\frac{J_1(\eta)}{\eta}d\eta, \tag{A 9}$$

$$\int_0^\eta \frac{1-J_0(z)}{z^2}dz = 1+O\left(\frac{1}{\eta}\right) \quad \text{as} \quad \eta\to\infty, \tag{A 10}$$

$$\int_0^\eta \frac{1-J_0(z)}{z}dz = O(\ln\eta) \quad \text{as} \quad \eta\to\infty, \tag{A 11}$$

$$0 < 1-J_0(\eta) < 2 \quad \text{for} \quad \eta > 0, \tag{A 12}$$

$$\int_0^\eta \frac{J_1(z)}{z}dz = 1+O\left(\frac{1}{\eta^{\frac{1}{2}}}\right) \quad \text{as} \quad \eta\to\infty. \tag{A 13}$$

Evaluation of w^*

From (A 3) and (A 8) we have

$$w^*(\lambda) = \frac{1}{\lambda}\int_0^\infty \frac{1-J_0(2K\lambda)}{K^2}f_{2,2}(K)\,dK. \tag{A 14}$$

Since $f_{2,2}(k) = 1+k\psi_{2,2}(k)$, both $f_{2,2}$ and $\psi_{2,2}$ satisfy the conditions (A 4)–(A 7). Then, using (A 10),

$$\begin{aligned} w^*(\lambda) &= \frac{1}{\lambda}\int_0^\infty \frac{1-J_0(2K\lambda)}{K^2}dK + \frac{1}{\lambda}\int_0^\infty \frac{1-J_0(2K\lambda)}{K}\psi_{2,2}(K)\,dK \\ &= 2+\frac{1}{\lambda}\int_0^\infty \frac{1-J_0(2K\lambda)}{K}\psi_{2,2}(K)\,dK + O\left(\frac{1}{\lambda}\right). \end{aligned} \tag{A 15}$$

Now, since $f_{2,2}$ and $\psi_{2,2}$ are bounded on $0 \leqslant K \leqslant \infty$, for $\lambda > 0$ and any given $m > 0$ we have

$$\begin{aligned} \left|\int_0^\infty \frac{1-J_0(2K\lambda)}{K\lambda}\psi_{2,2}(K)\,dK\right| &\leqslant \left[\int_0^m + \int_m^\infty\right]\left[\frac{1-J_0(2K\lambda)}{K\lambda}|\psi_{2,2}(K)|\right]dK \\ &\leqslant \sup_{K\in[0,m]}|\psi_{2,2}(K)|\int_0^m \frac{1-J_0(2K\lambda)}{K\lambda}dK \\ &\quad + \sup_{K\in[m,\infty]}|K\psi_{2,2}(K)|\int_m^\infty \frac{1-J_0(2K\lambda)}{K^2\lambda}dK \\ &= O(\lambda^{-1}\ln\lambda)+O(\lambda^{-1}), \end{aligned} \tag{A 16}$$

where we have used (A 10)–(A 12). Thence (A 15) and (A 16) yield

$$w^*(\lambda) = 2+O(\lambda^{-1}\ln\lambda). \tag{A 17}$$

Evaluation of $w_{1,i}$ $(i = 1, 2)$

Using (A 9), (A 10) can be rewritten as

$$w_{1,i}(\lambda) = 2\int_0^\infty \frac{f_{1,i}(K)}{K}dK\int_0^{2K\lambda}\frac{J_1(\eta)}{\eta}d\eta. \tag{A 18}$$

Now consider

$$w_{1,i} \equiv w_i^{\alpha}(\lambda; m) + w_i^{\beta}(\lambda; m) + w^{\gamma}(\lambda; m), \tag{A 19}$$

where

$$w_i^{\alpha}(\lambda; m) = 2\int_m^{\infty} \frac{f_{1,i}(K)}{K}\, dK \int_0^{2K\lambda} \frac{J_1(\eta)}{\eta}\, d\eta, \tag{A 20}$$

$$w_i^{\beta}(\lambda; m) = 2\int_0^{m} \psi_{1,i}(K)\, dK \int_0^{2K\lambda} \frac{J_1(\eta)}{\eta}\, d\eta, \tag{A 21}$$

$$w^{\gamma}(\lambda; m) = 2\int_0^{m} \frac{dK}{K} \int_0^{2K\lambda} J_1(\eta)\, d\eta \tag{A 22}$$

and m is an assigned positive parameter. Using (A 7)–(A 12),

$$w_i^{\alpha}(\lambda; m) = 2\int_m^{\infty} \frac{f_{1,i}(K)}{K}\, dK + O\left(\frac{1}{\lambda^{\frac{1}{2}}}\right). \tag{A 23}$$

Using (A 6), (A 12) and the boundedness of

$$\int_0^{\eta} J_1(z)\, dz/\eta \quad \text{for} \quad \eta \geqslant 0,$$

$$w_i^{\beta}(\lambda; m) = 2\int_0^{m} \psi_{1,i}(K)\, dK + O\left(\frac{1}{\lambda^{\frac{1}{2}}}\right). \tag{A 24}$$

Finally,

$$\begin{aligned} \tfrac{1}{2} w^{\gamma}(\lambda; m) &= \int_0^{2m} \frac{dz}{z} \int_0^{z\lambda} \frac{J_1(\eta)}{\eta}\, d\eta \\ &= \int_0^{2m} \frac{dz}{z} \int_0^{z} \frac{J_1(\eta)}{\eta}\, d\eta + \int_0^{\infty} \frac{dz}{z} \int_0^{z\lambda} \frac{J_1(\eta)}{\eta}\, d\eta - \int_{2m}^{\infty} \frac{dz}{z} \int_z^{z\lambda} \frac{J_1(\eta)}{\eta}\, d\eta. \end{aligned} \tag{A 25}$$

Here, using (A 12),

$$\int_0^{\infty} \frac{dz}{z} \int_z^{z\lambda} \frac{J_1(\eta)}{\eta}\, d\eta = \ln\lambda + O\left(\frac{1}{\lambda}\right). \tag{A 26}$$

The remaining two terms in (A 25) can be expressed as

$$\begin{aligned} &\int_0^{2m} \frac{dz}{z} \int_0^{z} \frac{J_1(\eta)}{\eta}\, d\eta - \int_{2m}^{\infty} \frac{dz}{z} \left[\int_z^{\infty} \frac{J_1(\eta)}{\eta}\, d\eta + O\left(\frac{1}{\lambda z}\right)^{\frac{1}{2}} \right] \\ &\quad = \int_0^{2m} \frac{J_1(\eta)}{\eta}\, d\eta \int_{\eta}^{2m} \frac{dz}{z} - \int_{2m}^{\infty} \frac{J_1(\eta)}{\eta} \int_{2m}^{\eta} \frac{dz}{z} + O\left(\frac{1}{\lambda^{\frac{1}{2}}}\right) \\ &\quad = \int_0^{\infty} \frac{J_1(\eta)}{\eta} [\ln 2m - \ln\eta]\, d\eta + O\left(\frac{1}{\lambda^{\frac{1}{2}}}\right). \end{aligned} \tag{A 27}$$

It follows that

$$\tfrac{1}{2} w^{\gamma}(\lambda; m) = \ln\lambda + [\ln 2m - A] + O(\lambda^{-\frac{1}{2}}), \tag{A 28}$$

where

$$A \equiv \int_0^{\infty} \frac{J_1(\eta)}{\eta} \ln\eta\, d\eta.$$

Combining (A 23), (A 24) and (A 28), we finally obtain

$$\tfrac{1}{2} w_{1,i}(\lambda) = \ln\lambda + \ln 2m - A + \mathscr{J}_m[f_{1,i}] + O(\lambda^{-\frac{1}{2}}), \quad i = 1, 2, \tag{A 29}$$

where

$$\mathscr{J}_m[f] \equiv \int_0^{m} \frac{f-1}{K}\, dK + \int_m^{\infty} \frac{f}{K}\, dK. \tag{A 30}$$

The m independence of (A 29) may readily be demonstrated by differentiation with respect to m. It does not, however, appear to be possible to express the result in a functional form independent of m. This is a consequence of the fact that the integrals

$$\int_0^m f_{1,i}(K)\,dK/K, \quad \int_m^\infty \psi_{1,i}(K)\,dK$$

do not exist.

Evaluation of W_1 and W_2

Inserting (A 27) and (A 30) into (A 1), we find

$$W_1(\lambda) = 2\ln\lambda + 2\{\ln 2m - A - \tfrac{1}{2} + \mathscr{J}_m[f_{1,1}]\} + O(\lambda^{-\frac{1}{2}}), \tag{A 31}$$

$$W_2(\lambda) = 2\ln\lambda + 2\{\ln 2m - A + 1 + \mathscr{J}_m[f_{1,2}]\} + O(\lambda^{-\frac{1}{2}}). \tag{A 32}$$

REFERENCES

BATCHELOR, G. K. 1970 Slender-body theory for particles of arbitrary cross-section in Stokes flow. *J. Fluid Mech.* **44**, 419.

BLAKE, J. R. 1971 A note on the image system for a stokeslet in a no-slip boundary. *Proc. Camb. Phil. Soc.* **70**, 303.

BLAKE, J. R. 1974 Singularities of viscous flow. Part 2. Applications to slender-body theory. *J. Engng Math.* **8**, 113.

BLAKE, J. R. & CHWANG, A. 1974 Singularities of viscous flow. Part 1. The image systems in the vicinity of a stationary no-slip boundary. *J. Engng Math.* **8**, 23.

COX, R. G. 1970 The motion of long slender bodies in a viscous fluid. Part 1. General theory. *J. Fluid Mech.* **44**, 791.

FAXÉN, O. H. 1923 Die Bewegung einer starren Kugel Längs der Achse eines mit zäher Flüssigkeit gefüllten Rohres. *Arkiv. Mat. Astr. Fys.* **17**, 27.

GRAY, J. & HANCOCK, G. J. 1955 The propulsion of sea urchin spermatozoa. *J. Exp. Biol.* **32**, 802.

HAPPEL, J. & BRENNER, H. 1965 *Low Reynolds Number Hydrodynamics.* Prentice-Hall.

KATZ, D. F. & BLAKE, J. R. 1974 Flagellar motions near walls. In *Proc. Symp. on Swimming and Flying in Nature.* (In press.)

LIGHTHILL, M. J. 1975 *Mathematical Biofluiddynamics.* Philadelphia: S.I.A.M.

MESTRE, N. J. DE 1973 Low-Reynolds-number fall of slender cylinders near boundaries. *J. Fluid Mech.* **58**, 641.

PIRONNEAU, O. & KATZ, D. F. 1974 Optimal swimming of flagellated micro-organisms. *J. Fluid Mech.* **66**, 391.

TILLET, J. P. K. 1970 Axial and transverse Stokes flow past slender axisymmetric bodies. *J. Fluid Mech.* **44**, 401.